Oil Shale, 2009, Vol. 26, No. 2, pp. 125–138
doi: 10.3176/oil.2009.2.05
ISSN 0208-189X

NUMERICAL SIMULATION OF UPRISING GAS-SOLID PARTICLE FLOW IN CIRCULATING FLUIDISED BED

A. KARTUSHINSKY[(a)*], A. MARTINS[(a)], Ü. RUDI[(a)], I. SHCHEGLOV[(a)], S. TISLER[(a)], I. KRUPENSKI[(b)], A. SIIRDE[(b)]

[(a)] Tallinn University of Technology
Faculty of Science, Laboratory of Multiphase Media Physics
Akadeemia tee 21E, 12618 Tallinn, Estonia

[(b)] Tallinn University of Technology
Faculty of Mechanical Engineering, Department of Thermal Engineering
Kopli 116, 11712 Tallinn, Estonia

Concentration of solid particles of ash and inert material present in the combustion chamber of a circulating fluidised-bed boiler is very high, giving rise to some disadvantages. At the same time, the required temperature level in the combustion chamber is guaranteed by circulation of solid particles. In this work numerical simulation of gas-solid particle flow has been performed in the frame of a two-fluid model, namely the Eulerian approach for the dispersed phase, for conditions of the circulating fluidised bed, ranging from moderate to high mass ratios of the flow. An incorporated original model of closure of transport equations of the dispersed phase permitted to account the interparticle collisions which might be indispensable to proper numerical simulation of the process in the circulating fluidised bed under discussion. The results of this work would help to improve the processes occurring in the combustion chamber of the circulating fluidised-bed boiler.

Introduction

In accordance with widespread introduction of circulating fluidised-bed (CFB) furnaces in power plants, the concentration of solid ash particles in flue gas substantially increases. Ash particles in flue gas of the pulverised firing boilers can be observed as an inconvenient admixture. These particles pose specific problems, such as the behaviour of inorganic matter in the combustion process, fouling, high-temperature corrosion and wear of the steam boiler heating surfaces. In CFB furnaces solid ash particles are used mainly as the solid heat carrier – separated in a hot cyclone and cooled in a

* Corresponding author: email *aleksander.kartusinski@ttu.ee*

heat exchanger, ash particles return into the furnace. Temperature level in the furnace is held in the given range by the circulating ash mass. While the heat capacity of ash is quite low, the circulating ash mass must be high. High ash concentration in flue gas is attained (a) by high velocity of gas in the bed and by the fact that most of fuel particles carried out of the bed are burnt and their ash fills the whole volume of the furnace, and (b) by ash circulation. The CFB combustion technology enables to bind sulphur components with carbonate components added to the fuel or existing within the mineral part of the fuel.

A disadvantage of CFB boilers is that some fuel ash particles become too fine during circulation, and therefore the size of ash particles present in flue gas exiting the hot cyclone is too small. As a result of disintegration, the mass of the fine ash particles, which are not separated from flue gas or occur in the connective flue ducts and in the multicyclone, increases. High concentration of particles in flue gas of the CFB furnace chamber contributes to the formation of particle clusters with the solid phase concentration within 0.1–0.2 m^3/m^3. At the exit of the CFB boiler furnace, density of the solid phase is within 5–20 kg/m^3 [1].

Numerical simulations are mainly performed within the Lagrangian approach by tracking of single particles or their packages in order to capture particle-fluid interactions. For example, the two-dimensional gas-solid particle flow taking place in the CFB riser with a total volume concentration of solids 3% has been studied in [2] by the Lagrangian approach using the method of particle tracking.

In the present study the two-fluid model, i.e. the Eulerian approach, is applied to describe the motion of the dispersed phase. The advantage of the Eulerian method is the possibility to obtain the distributions of all dynamic parameters of the flow, including the particle mass concentration. This method does not depend on the number of the tracked particles which model the motion of the disperse phase, contrary to the Lagrangian approach, at which convergence is determined by the number of the tracked single particles that can be up to hundreds of thousands, and it requires high computational capabilities.

The implementation of an original closure model of linear and angular momentum of polydispersed solid phase [3, 4] based on interparticle collision in Eulerian frame allows, first of all, to describe correctly the four-way coupling effect in the case of highly loaded flow, second, to take into account collisions of the particles, which seem to be very significant with respect to the high flow mass ratio and wide range of the particle size deviation.

Our model [5] was applied for the pneumatic transport in the case of fluidized bed: $T = 850$ °C, low density of carrier gas $\rho = 0.27$ kg/m^3, high coefficient of kinematic viscosity which is roughly 10 times larger than that in the normal conditions and the real inlet size of 2.5 m.

Within the Eulerian approach, the original collision model was used for the closure of transport equations by accounting the interparticle collision effect occurring in CFB due to high mass loading [6].

The numerical parametric study deals with the influence of parameters of various riser exits on the hydrodynamics of the gas-solid two-phase flow taking place in the riser of CFB [7]. The problems of two-phase flows in the CFB risers are analysed in publications, but these studies do not consider the dependence of the amount of the sensible heat carried by solid ash particles on their concentration in gases.

In the present work the gas-solid particle flow in conditions of CFB is studied, taking into account the amount of heat, which must be separated from the combustor by the sensible heat of the solid ash particles. This approach enables to optimize the concentrations of the solid ash particles in flue gas.

Basic terms of calculations

For numerical simulation of the uprising gas-solid particle flow in the vertical riser under the CFB conditions, namely temperature, gas velocity, and particle concentration were calculated. The particles of the Estonian oil shale ash of a certain density and size were chosen as the dispersed phase.

The following simplifications were applied for numerical simulations of the uprising gas-solid particle flow: 1) the calculations concern the upper part of the furnace, before the exit region, 2) the cross-section of the furnace is circular, 3) flue gas contains only solid ash particles taking part in the circulation process, 4) actual gas velocity was chosen equal to 5.5 m/s [8] and 5) small-size and coarse ash particles of three different particle-size ranges were chosen for calculations.

Table 1 presents the initial data used in the calculations.

Taking into consideration the part of heat, which must be separated from the furnace by fly ash, the volumetric concentration of the solid phase present in flue gas at the exit of the CFB boiler furnace can be calculated as follows:

$$\rho_s = q_k \eta Q_i^r / \left[V_g + (a-1)V_0 \right] \eta_c \Delta c \text{ , kg}_{\text{ash}}/\text{nm}^3. \quad (1)$$

Equation (1) can be simplified. When the excess air coefficient at the exit of the CFB boiler furnace is 1.25, the ratio of different solid fuels is $Q_i^r / \left[V_g + (a-1)V_o \right] \approx 2.43–2.88$ MJ/nm^3 [7]. If the fly ash temperature at the exit of the CFB boiler furnace is 850 °C and after the ash cooler it equals 600 °C, $\Delta c = 0.264$ MJ/kg$_{\text{ash}}$. The simplified formula looks as follows:

$$\rho_s \approx q_k \eta \eta_c \text{ , kg}_{\text{ash}}/\text{nm}^3. \quad (2)$$

As follows from Eq. (2), in theory the whole fuel heat could be separated from the furnace by the solid fly ash particles ($q_k = 100\%$, $\eta = 90\%$, $\eta_c = 95\%$), when the volumetric concentration of the solid phase in flue gas at the exit of the CFB boiler furnace is about 9.5 kg$_{\text{ash}}$/nm^3. It means that

Table 1. **The initial data for calculations of the CFB vertical riser**

Parameter	Value	
Flue gas temperature, °C	850	
Flue gas velocity, m/s	5.5	
Flue gas density, kg/nm^3	0.27	
Density of ash particles, kg/nm^3	1300	
Volumetric concentration of the solid phase (ash):		
low, m^3/nm^3; kg/nm^3	0.0003; 1.4	
high, m^3/nm^3; kg/nm^3	0.0021; 10.0	
Granular composition of ashes	Particle size range, mm	Percentage, %
Small-size ash	0–0.02	50
	0.02–0.03	30
	0.03–0.05	20
Coarse ash	0–0.2	50
	0.2–0.4	30
	0.4–0.7	20

practically the volumetric concentration of the solid phase in flue gas at the exit of the CFB boiler furnace must be substantially less than 10 kg_{ash}/nm^3. For example, in Lurgi Lentjes Bischoff (LLB) CFB 100 MW_{th} project, circulating fly ash separated 18% of the fuel heat from the furnace. The boiler efficiency is 91% [8] and the cyclone ash separation efficiency is 95%. The volumetric concentration of the solid phase in flue gas at the exit of the CFB boiler furnace calculated by Eq. (2) must be 1.72 kg_{ash}/nm^3.

For the calculations the volumetric concentration of the solid phase in flue gas at the exit of the CFB boiler furnace was chosen equal to 1.4 and 10 kg/nm^3 (see Table 1) on the basis of the estimations presented above.

The turbulent boundary layer model

The numerical simulation has been performed within the framework of the two-phase turbulent boundary layer (TBL) approach. This implies that the diffusive source terms were retained in one direction only, namely in transverse one, and magnitudes of the average transverse velocity components of the gas- and dispersed phases were much less than those of the longitudinal components of the corresponding velocities of both phases. Such approach is thoroughly valid and used in the case of pipe channel flows as well as in the turbulent round jets together with the flow past of the rigid shapes [3, 9, 10].

The two-fluid model was applied for calculations assuming the dispersed phase to be the continuous phase, but having its own flow parameters such as the velocities, concentration, etc., which differ from those of the carrier fluid. Actually, the dispersed phase is polydispersed, therefore its motion was modelled by the motion of the finite number of particle fractions. In order to simplify the numerical simulations three particle fractions were

considered. They were characterized by their own mass fractions and particle sizes in order to take into account the interparticle collisions along with other force factors [4, 5]. The collision effect was characterized here by introducing the so-called pseudo-viscosity coefficients, ν_{ci}, D_{ci}, the diffusion coefficient of particles D_{ci} depending from their collisions and being similar to the coefficient of the turbulent diffusion of particles in the differential equation of the particle mass conservation (Eq. (4)). These pseudo-viscosity coefficients were calculated analytically by the model [4]. Among the other force factors included in the model there were the drag force determined by the particle response time, τ_i, the lift Magnus and Saffman forces characterized by the angular velocity slip between gas and dispersed phase, $\Omega_i = \frac{1}{2}\frac{\partial u}{\partial r} - \omega_{si}$, the gravitation force designated by the gravitation acceleration, g. The four-way coupling model by [11] was applied. It means that the particles are also involved into turbulent motion of the carrier fluid. This involvement was described by the coefficient ν_{si}.

It allowed to take into account both generation and attenuation of turbulence of gas by particles.

The governing TBL equations presented in the tensor form are the following (here "i" is the number of the particle fractions, i = 1,3):

$$\frac{D\rho}{Dt} = 0\,, \tag{3}$$

$$\frac{Du_j}{Dt} = \frac{\partial}{r\partial r} r\left(\nu_t + \nu\right)\frac{\partial u_j}{\partial r} - \frac{\partial p}{\rho \partial x} - \sum_{i=1,3} \alpha_i \left\{ C'_{Di} \frac{\left(u_j - u_{sij}\right)}{\tau_i} + C_{Mi}\left[\vec{\Omega}_i \times \left(\vec{v} - \vec{v}_{si}\right)\right]_j \right\}, \tag{4}$$

$$\frac{Dk}{Dt} = \frac{\partial}{r\partial r} r\left(\nu_t + \nu\right)\frac{\partial k}{\partial r} + \frac{G}{\rho} - \frac{\varepsilon_0}{\rho} + \sum_{i=1,3} \frac{\alpha_i}{\tau_i}\left[(u_j - u_{sij})^2 + k_{sci} - \left\langle u'_j u'_{sij} \right\rangle\right], \tag{5}$$

$$\frac{D\rho\alpha_i}{Dt} = 0, \tag{6}$$

$$\frac{D\alpha_i u_{sij}}{Dt} = \frac{\partial}{r\partial r} r\alpha_i \left(\nu_{si} + \nu\right)\frac{\partial u_{sij}}{\partial r} - \frac{\partial p_{ci}}{\rho \partial x} + \alpha_i \left\{ C'_{Di} \frac{\left(u_j - u_{sij}\right)}{\tau_i} + C_{Mi}\left[\vec{\Omega}_i \times \left(\vec{v} - \vec{v}_{si}\right)\right]_j - \left(1 - \frac{\rho}{2\rho_p}\right) g \right\}, \tag{7}$$

$$\frac{D\alpha_i \omega_{si}}{Dt} = \frac{\partial}{\partial r} r\alpha_i \left(\nu_s + \nu_{ci}\right)\frac{\partial \omega_{si}}{\partial r} + \frac{\Omega_i}{\tau_i} k_\omega. \tag{8}$$

Here Eq. (3) is the continuity equation, Eq. (6) is the mass conservation equation of the polydispersed phase, Eqs. (4) and (7) presented in the tensor form cover the momentum exchange for the longitudinal and radial directions for the gas and polydispersed phases, respectively. Eq. (8) presents the angular momentum exchange, the coefficient $k_\omega = \frac{10}{3}$.

The closure of the momentum equations was performed by the transport equation of the turbulent energy (Eq. (5)) derived by [11].

Results and discussion

The influence of the solid phase concentration

The behaviour of particles with high and low phase concentration is different, as shown in Figs. 1–4. It is known that the increase of the particle mass concentration as well as the decrease of the particle size results in the decrease of the velocity slip between gas and dispersed phases [10], which is indirectly expressed *via* the profiles of the radial velocity component of the dispersed phase obtained for the motion of relatively small particles of 25 μm at the high flow mass ratio (bold solid line, Fig. 3) *versus* the distribution of the same velocity at the low mass ratio (solid line, Fig. 3). The effect of the mass ratio is mostly pronounced in the profile of the turbulent energy as the low level of turbulence at the high flow mass ratio (solid bold line, Fig. 2) *versus* the higher level of turbulence at the low mass loading (solid line, Fig. 2), that is called the turbulence modulation due to the presence of the particles in the flow. The small changes of the axial velocity and the mass concentration profiles can be seen in Figs. 1 and 4, respectively, for various flow mass ratios.

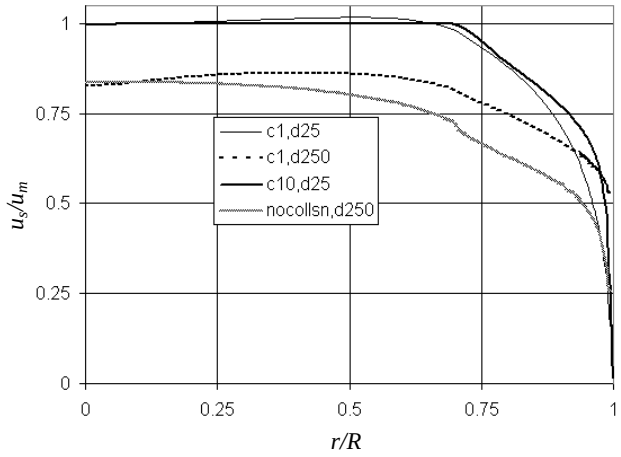

Fig. 1. Axial velocity profiles of the dispersed phase for different particle sizes: δ = 25 μm (d25), δ = 250 μm (d250) and various mass ratios: c = 1 kg/kg (c1), c = 10 kg/kg (c10) with and without particles collision effect (no collision).

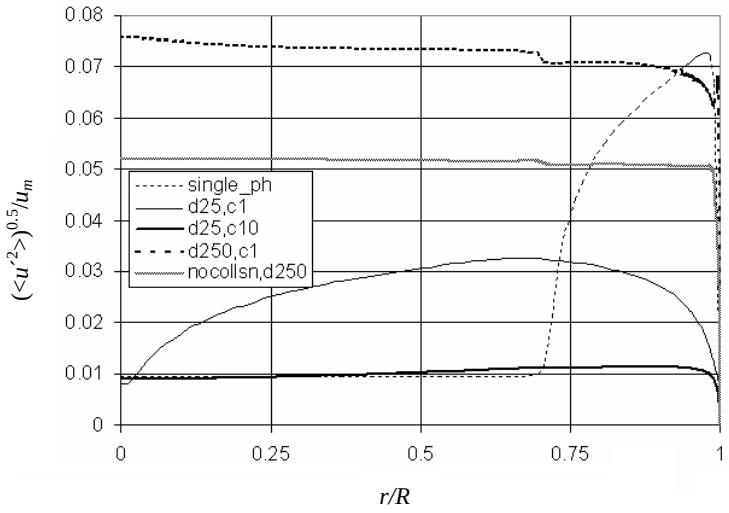

Fig. 2. R.m.s profiles of velocity of carrier fluid for different particle sizes: δ = 25 μm (d25), δ = 250 μm (d250) and various mass ratios: c = 1 kg/kg (c1), c = 10 kg/kg (c10) with and without particles collision effect (no collision).

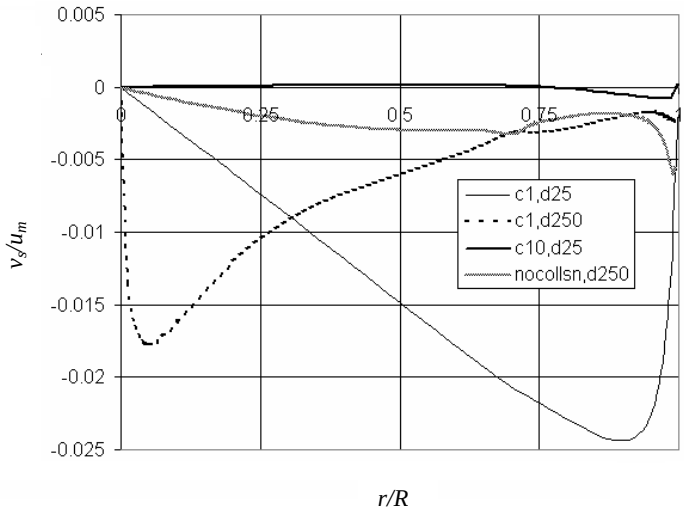

Fig. 3. Radial velocity profiles of particles for different particle sizes: δ = 25 μm (d25), δ = 250 μm (d250) and various mass ratios: c = 1 kg/kg (c1), c = 10 kg/kg (c10) with and without particles collision effect (no collision).

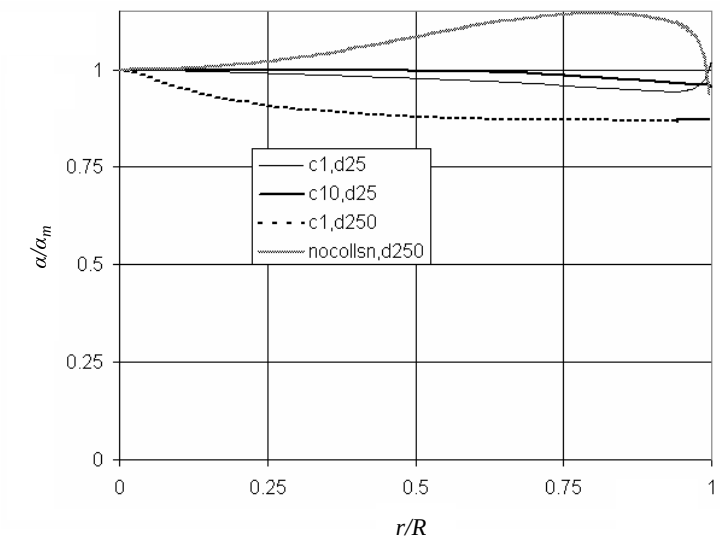

Fig. 4. Profiles of particle mass concentration for different particle sizes: δ = 25 μm (d25), δ = 250 μm (d250) and various mass ratios: c = 1 kg/kg (c1), c = 10 kg/kg (c10) with and without particles collision effect (no collision).

The influence of the particle size

The effect of the particle size is expressed by the distribution of the axial velocity component of the particles obtained at the same mass ratio of 1 kg dust/kg air for relatively small 25 μm and coarse 250 μm particles (Fig. 1), namely, smaller particles have higher level (solid line) that those of larger ones (bold dotted line). With respect to the distribution of the radial velocity component, small particles have higher velocity in the vicinity of the wall (solid line, Fig. 3) in contrast to the velocity growth occurring close to the axis in the case of a motion of large particles (bold solid line, Fig. 3). This is due to the stronger Magnus effect of the lift force causing lag motion of large particles shifting them towards the axis. The manifest effect of the particle size is expressed *via* the distribution of the turbulent energy, namely, larger particles generate higher additional turbulent energy due to the vortex shedding than those of smaller ones (cf. bold dotted line and solid line, Fig. 2). The mass profiles of the small and coarse particles are slightly different, i.e. the concentration of small particles has less gradient than coarse particles (cf. bold dotted line for large and solid line for small particles, Fig. 4).

The interparticle collisions

The effect of the interparticle collisions is important for the particulate flows of the mass ratio larger than 1 kg dust/kg air, when $\tau_c / \tau < 1$, where the time of interparticle collision τ_c is less than the particle response time τ. The

calculations were run taking into account the interparticle collisions described by the pseudo-viscosity coefficients (Eq. (7)), using the original model of the closure based on the particle collisions [4]. To show the importance of this effect, one set of the calculations was performed neglecting the particle collisions (cf. bold dotted and pale lines, Fig. 1) in the case of the motion of the rough 250 μm particles while comparing the profiles of the axial velocity of the dispersed phase with the mass ratio of 10 kg dust/kg air. The change of these profiles is obvious, namely, in the case of no collision the axial velocity profile becomes narrower that is related to the reduction of the particle diffusion in the radial direction caused by the interparticle collisions [4, 5]. Besides, the collision effect results in additional turbulence generation derived from the four-way coupling model by [11] (cf. bold dotted and pale lines, Fig. 2).

The distribution of the radial velocity of the dispersed phase shows that the absence of collisions diminishes the Magnus lift force due to the less velocity slip and therefore the less value of the radial velocity of particles (cf. bold dotted and pale lines, Fig. 3). Finally, the neglect of collisions leads to a growth of concentration in the wall vicinity (cf. pale line *versus* bold dotted line, Fig. 4), because of underestimating of diffusion of particles.

As a whole, the interparticle collisions generate high turbulence and, thus, contribute to the better mixing of particles.

Development of upward motion of particles in the vertical riser

In order to follow the two-phase flow development, the calculations were started from the uniform distribution of parameters of the dispersed phase, namely velocity and concentration, set in the initial cross-section and continued up to the exit cross-section (the whole length was equalled 6 calibres of the riser). Figs. 5–7 show the results obtained for the middle cross-section (dotted and bold dotted lines) and for the outlet cross-section (solid and bold solid lines) for small 25 μm and coarse 250 μm particles. One can see that small particles have high rate of acceleration with the distinct difference of the velocity distributions along the x axis of the riser in contrast to the motion of coarse particles which are characterized by slightly differing velocity distributions due to short length (6 calibres) and high inertia of particles (cf. bold solid and bold dotted lines, Fig. 5). With respect to the radial velocity component which is responsible for the momentum exchange one can notice that the velocity in the middle cross-section is higher (dotted line) than that at the exit cross-section (solid line). Such change in the velocity is observed in the case of motion of the coarse 250 μm particles (cf. bold dotted and bold solid, Fig. 6). This is due to the gradual adjusting of motion of the dispersed phase to the flow conditions of the gas phase, however this is the coupling process. Finally normalised root mean square (r.m.s.) velocity of the gas phase is fitted to the flow conditions downstream, so small particles reduce the initial high level of turbulence due to artificial set as uniform velocity distribution in the inlet cross-section (cf.

profiles with dotted line and solid line, Fig. 7), and in the case of motion of coarse particles, the turbulent energy in terms of the r.m.s distribution slightly changes from the middle to the outlet cross-section (cf. bold dotted and bold solid lines, Fig. 7).

Thus, the parameters of the dispersed phase artificially set in the inlet cross-section are modified to fit the flow conditions downstream.

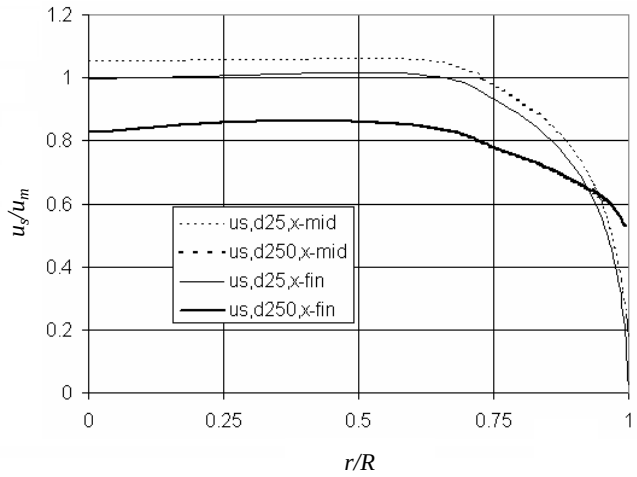

Fig. 5. Progress of axial particle velocity along the height with collision effect in the middle cross-section (x-mid) and in the flow exit (x-fin) at the motion of different particles: δ= 25 μm and δ=250 μm.

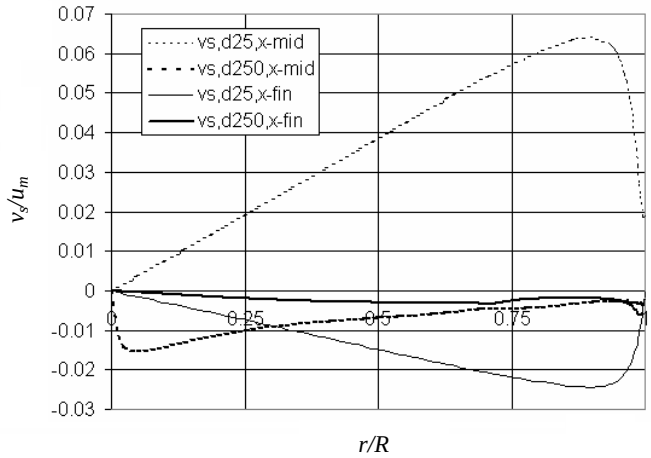

Fig. 6. Progress of radial particle velocity along the height with collision effect in the middle cross-section (x-mid) and in the flow exit (x-fin) at the motion of different particles: δ= 25 μm and δ= 250 μm.

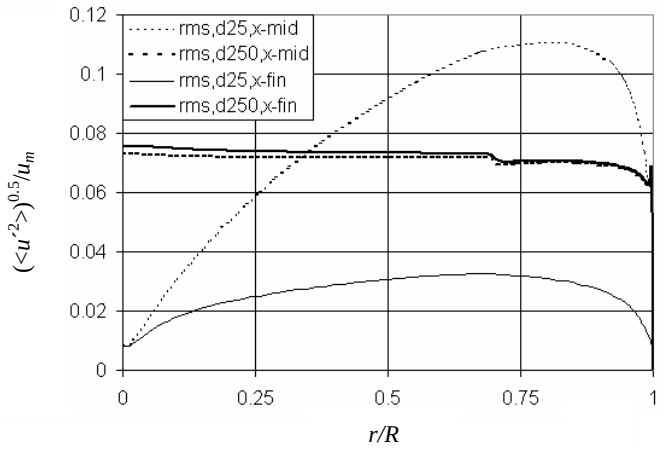

Fig. 7. Progress of r.m.s. velocity along the height with collision effect in the middle cross-section (x-mid) and in the flow exit (x-fin) at the motion of different particles: δ = 25 μm and δ = 250 μm.

Conclusions

On the basis of the performed calculations one can draw the following conclusions:

- interparticle collisions generate high turbulence and contribute to better particle mixing and enhance the heat exchange between solid ash particles and gases;
- low particle mass concentration results in high velocity of both phases and high level of turbulence;
- large level of velocity slip at the motion of coarse particles all over the flow domain results in enhancement of the turbulence of the carrier fluid;
- the modelling states that the optimal concentration can be achieved with the guaranteed interparticle collisions, and further increasing of the mass loading would not be desirable.

Recommendations

The results of this work permit to propose the following recommendations to improve the processes occurring in the furnace of CFB:

- concentration of solid ash particles in flue gas must be decreased in optimal way; it means that the required temperature of flue gas and the interparticle collisions must be guaranteed;
- the interparticle collisions take place when the volumetric concentration of the solid phase (ash) is higher than 1 kg/m^3;

- at the exit of the CFB boiler furnace the volumetric concentration of the solid phase (ash) must be lower than 10 kg/m^3. It means that at the exit of the CFB boiler the volumetric concentration of the solid phase (ash) must be in the range of 1–10 kg/m^3.

Acknowledgement

The work was supported by a Grant No. ETF7620 of Estonian Science Foundation and by the target financing SF0140070s08.

Nomenclature

Roman Symbols

a – excess air coefficient;
C'_D – factor of drag coefficient;
C_M – coefficient of Magnus force;
C_ω – coefficient of torque;
c – particle mass loading of a flow, kg/kg;
c_{ls} – sensible heat of separated hot, MJ/kg$_{ash}$;
c_{lv} – sensible heat of cooled fly ashes, MJ/kg$_{ash}$;
D_{ci} – pseudo-viscosity coefficient of particles originated from interparticle collisions, m^2/s;
G – turbulence generation originated from nonuniform distribution of fluid velocity, m^2/s^3;
g – gravitational acceleration, m/s^2;
k – turbulent energy, m^2/s^2;
k_s – energy of dispersed phase due to particles' collision, m^2/s^2;
k_{sci} – kinetic energy of dispersed phase originated from interparticle collisions, m^2/s;
k_ω – ratio between the response time of torque and linear momentum of dispersed phase;
p – pressure, kg/m^2;
p_{ci} – pressure of the dispersed phase originated from interparticle collisions, kg/m^2;
Q_i^r – calorific value of fuel as received, MJ/kg;
q_k – part of heat, separated from furnace with sensible heat of fly ash, %;
R – pipe radius, m;
r – radial coordinate, m;
T – temperature of fluidized bed, $^\circ$C;

t – time period, s;
u – axial velocity component of fluid, m/s;
$\overline{u}$ – fluid velocity over cross-section, m/s;
u_m – axial velocity of fluid at the flow centre line, m/s;
u_s – axial velocity component of dispersed phase, m/s;
$\left\langle u'_j u'_{sij} \right\rangle$ – velocity correlation between fluid and dispersed phase, m^2/s^2;
V_0 – theoretical amount of air for combustion of one kg fuel, nm^3/kg;
V_g – amount of the flue gas raised during combustion of one kg fuel, nm^3/kg;
v – radial velocity component of fluid, m/s;
v_s – radial velocity component of dispersed phase, m/s;
x – axial coordinate, m;
$\langle\ \rangle$ – averaging procedure.

Greek Symbols

α – particle mass concentration, kg/kg;
Δc – difference of sensible heat of separated hot and cooled fly ashes, MJ/kg_{ash};
δ – particle diameter, μm;
ε – dissipation rate of turbulent energy, m^2/s^3;
η – boiler efficiency, %;
η_c – cyclone ash separation efficiency, %;
ν – kinematic viscosity coefficient of fluid, m^2/s;
ν_{ci} – pseudo-viscosity coefficient of particles originated from interparticle collisions, m^2/s;
ν_{si} – pseudo-viscosity coefficient of particles originated from particles involvement into turbulent motion, m^2/s;
ν_t – turbulent viscosity coefficient of fluid, m^2/s;
ρ – density of gas, kg/m^3;
ρ_p – particle material density, kg/m^3;
ρ_s – volumetric concentration of dispersed phase, kg_{ash}/nm^3;
τ – particle response time, s;
τ_c – time of interparticle collision, s;
Ω_i – angular velocity slip between gas and dispersed phases, 1/s;
ω_{si} – angular particles velocity, 1/s.

Subscripts

i – i-th particle fraction of dispersed phase;
j – j-th particle fraction of dispersed phase.

REFERENCES

1. *Ots, A.* Oil Shale Fuel Combustion. – Tallinn, 2006.
2. *Helland, E., Occelli, R., Tadrist, L.* Numerical study of cluster formation in a gas-particle circulating fluidised bed // Powder Technol. 2000. Vol. 110, No. 3. P. 210–221.
3. *Frishman, F., Hussainov, M., Kartushinsky, A., Mulgi, A.* Numerical simulation of a two-phase turbulent pipe-jet flow loaded with polyfractional solid admixture // Int. J. Multiphase Flow. 1997. Vol. 23, No. 4. P. 765–796.
4. *Kartushinsky, A., Michaelides, E. E.* An analytical approach for the closure equations of gas-solid flows with inter-particle collisions // Int. J. Multiphase Flow. 2004. Vol. 30, No. 2. P. 159–180.
5. *Kartushinsky, A., Michaelides, E. E.* Gas-solid particle flow in horizontal channel: decomposition of the particle-phase flow and inter-particle collision effect // J. Fluids Eng. 2007. Vol. 129, No. 6. P. 702–712.
6. *Hussain, A., Ani, F. N., Darus, A. N., Mustafa, A., Salema, A. A.* Simulation studies of gas-solid in the riser of a circulating fluidized bed // Proceedings of the 18th International Conference on Fluidized Bed Combustion, ASME Publication, 2005. Article No. FBC2005-78014. P. 201–207.
7. Thermal Calculation of Power Generators (Standard Method). – Moscow, Energija, 1973 [in Russian].
8. Oil Shale Perspectives Within Energy Production, Estonia. Outline Proposal for 100 MW_{th} Demonstration CFB Boiler. – Lurgi Energie und Umwelt GmbH, Frankfurt am Main, 1995.
9. *Hussainov, M., Kartushinsky, A., Mulgi, A., Rudi, Ü., Tisler, S.* Experimental and theoretical study of the distribution of mass concentration of solid particles in the two-phase laminar boundary layer on a flat plate // Int. J. Multiphase Flow. 1995. Vol. 21, No. 6. P. 1141–1161.
10. *Hussainov, M., Kartushinsky, A., Mulgi, A., Rudi, Ü.* Gas-solid flow with the slip velocity of particles in a horizontal channel // J. Aerosol Sci. 1996. Vol. 27, No. 1. P. 41–59.
11. *Crowe, C. T., Gillandt, I.* Turbulence modulation of fluid-particle flows – a basic approach // Proceedings of the 3rd International Conference on Multiphase Flow, Lyon, France, June 8–12, 1998. CD-ROM.

Received October 8, 2008